Numerical Analysis of the Flow Between a Pair of Corotating Enclosed Disks

Joan Herrero and *Francesc Giralt*, Universitat Rovira i Virgili de Tarragona, Departament d'Enginyeria Química, Tarragona, Catalunya, Spain, and *Joseph A. C. Humphrey*, University of Arizona, Department of Aerospace and Mechanical Engineering, Tucson, Arizona, USA

Introduction

Many mechanical devices involving engineering applications contain rotating disks. The presence of a large, flat surface together with a rotation-induced fluid motion makes this geometrical system suitable for the transfer of heat, mass and momentum. The problem is relevant not only at a fundamental level in fields such as geophysics but in engineering practice as well. Rotating disks are present, for example, in turbomachinery, reactors for the manufacture of semi-conductors by chemical vapour deposition (CVD), rotating disk contactors for liquid-liquid extraction, rotating disk electrodes, etc.

The flow between a pair of corotating disks in a fixed enclosure has received a great deal of attention in recent years because it approximates the geometry of magnetic information storage devices in the computer industry (more commonly known as 'hard disks'.) A sketch of the problem investigated is shown in Fig. 1. The most relevant geometrical parameter is the height to radius aspect ratio, $\Gamma = H / (R_2 - R_1)$, where H is the inter-disk axial spacing and R_1, R_2 are the disk inner and outer radius, respectively. A review of the literature on the subject prior to 1991 can be found in the article by Humphrey et al. [1]. At relatively low rotation speeds, i.e., low values of the Reynolds number, $Re = \Omega R_2^2 / n$, the flow between a pair of corotating disks in a fixed enclosure is steady, axisymmetric (2D) and is characterised by a pair of counter-rotating cross-stream vortices near the outer cylindrical wall [2-4]. In the above expression for the Reynolds number W is the angular velocity of rotation of the disks and hub, R_2 is the disk external radius and v is the fluid kinematic viscosity.

When the angular velocity of rotation of the disks and hub is sufficiently increased, the flow becomes three-dimensional (3D) and unsteady. Such a 2D-3D transition was already reported in early investigations such as, for example, that of Lenneman [5]. More recently, Humphrey et al. [6] analysed numerically the 3D structure of the flow at a height to radius aspect ratio of $\Gamma = 0.2$. The flow displays a 3D wavy structure which precesses with respect to the disks and hub. The wavy nature of the flow leads to a fluctuating behaviour of the measured or computed velocity records, which are observed to oscillate around its average value. The contribution by Humphrey et al. [6] does not account, however, for all of the complexities of the 3D flow reported in some of the previous experimental investigations, such as that of Abrahamson et al. [7]. A more comprehensive analysis of the structure of the 3D flow in the range of aspect ratios $0.1 \leq \Gamma \leq 0.4$ may be found in the contribution by Herrero et al. [8], who also assessed the effect of a radial clearance between the disk tip and the enclosure wall (see Fig. 1.)

In the remainder of the text, conservation equations governing the flow can be found in Section 2, the main features of the numerical algorithm are discussed in Section 3 and finally Section 4 presents some examples of the calculations carried out by the authors over the period 1993-1996.

Conservation equations

The flow is assumed to be incompressible, laminar and Newtonian. In these conditions, the conservation of mass and momentum in a frame of reference rotating at the angular velocity of rotation of the disks and hub, Ω, is governed by the following set of partial differential equations:

continuity:

$$\frac{\partial u}{\partial z} + \frac{\partial v}{\partial r} + \frac{v}{r} + \frac{1}{r}\frac{\partial w}{\partial \theta} = 0 \qquad (1)$$

z-momentum:

$$\frac{D\,u}{D\,t} = -\frac{1}{\rho}\frac{\partial\,p'}{\partial\,z} + \nu\,\nabla^2 u \qquad (2)$$

r-momentum:

$$\frac{D\,v}{D\,t} = -\frac{1}{\rho}\frac{\partial\,p'}{\partial\,r} + \nu\,\nabla^2 v + \qquad (3)$$
$$+ \Omega^2 r + 2w\Omega + w^2/r$$

θ-momentum:

$$\frac{D\,w}{D\,t} = -\frac{1}{r\,\rho}\frac{\partial p'}{\partial \theta} + \nu\,\nabla^2 w - \qquad (4)$$
$$- \left(2v\Omega + vw/r\right)$$

where ρ is the fluid density, u, v, and w are the respective velocity components in the axial, radial and circumferential directions (z, r, θ), t denotes time, p' is the modified pressure (which also includes the contribution of the gravity potential field,) the symbol D/Dt denotes the substantial derivative and ∇^2 stands for the Laplacian operator. Some terms in the above equations arise as a result of the rotation of the frame of reference and play a major role in determining the structure and the stability properties of the flow under investigation. These are the centrifugal force ($\Omega^2 r$) in Eq. (3) and the radial ($2w\Omega$) and circumferential ($-2v\Omega$) components of the Coriolis force in Eqns. (3) and (4). The above conservation equations are subject to the following set of boundary conditions:

$$u = v = 0 \text{ at any solid boundary} \qquad (5a)$$

$$w = 0 \text{ at the disk and hub surfaces} \qquad (5b)$$

$$w = -\Omega R_2 \text{ at the enclosure wall} \qquad (5c)$$

It should be noted that the Eqns. (2-4) are given in dimensional form. The corresponding non-dimensional equations can be obtained by introducing R_2 and ΩR^2 as the respective length and velocity scales and defining the corresponding dimension-

less variables. The Reynolds number, defined in Section 1 above, would therefore appear in the resulting dimensionless equations.

Numerical method

Calculations have been performed using the CUTEFLOWS numerical algorithm for unsteady incompressible flows [6]. It has been extensively tested and successfully used to calculate a variety of flow configurations including rotating disk, bluff bodies [9, 10], and backward-facing step [11, 12] problems. The algorithm is based on a staggered-grid, control volume discretization approach to derive finite difference forms of the conservation equations in terms of primitive variables. Central differencing is used to approximate the pressure and diffusion terms in the momentum equations. The second order accurate QUICK scheme is used for the convection terms. Continuity yields a discrete Poisson equation which is solved for pressure using the conjugate gradient method. The algorithm is explicit in time and the use of a second order Runge-Kutta scheme renders it second order accurate in time as well as in space. The explicit character of the time-marching makes possible a high degree of vectorization and parallelization of the code.

The distribution of computational nodes throughout the calculation domain is optimised so that the grid is fine enough in the vicinity of any solid boundary, where strong velocity gradients occur. The amount of computational nodes in a typical 3D calculation ranges from 150,000 to 300,000, depending on the particular conditions of a given run. The total CPU time required for a complete calculation also depends on the characteristics of each run. Typical CPU times (on the basis of 1 CPU on a CRAY-YMP computer) for a 3D run range between 20 and 200 hours.

Results

Results presented here correspond to the case with $\Gamma = 0.2$ and $A = 0$ (see Fig 1.) At this height to radius aspect ratio, which matches that of Schuler's [13] experimental device, transition from steady 2D to unsteady 3D flow is numerically detected at a Reynolds number about Re = 16,000. Changes in Γ lead to important modifications in the value of the transition Reynolds number as well as in the structure of the resulting 3D flow [8].

At any Reynolds number value below the 2D-3D transition boundary the flow is steady and axisymmetric. The typical cross-stream structure of this 2D flow is shown in Fig. 2, where streamlines are plotted for a calculation at Re = 13,710 on a 40x74 (z, r) computational grid. When the Reynolds number is increased beyond the critical value the flow becomes 3D and unsteady and the cross-stream vortices acquire a wavy shape. This is shown in Fig. 3a, where the instantaneous cross-stream structure of the flow at a given circumferential location is plotted for a 3D calculation with Re = 20,565 on a 40x74x52 (z, r, θ) grid. The oscillation of the cross-stream flow structure also affects the main, circumferential motion, as illustrated in Fig. 3b where the distribution of the axial component of vorticity (basi-

cally a function of w only) is plotted for the same conditions of Fig. 3a. The oscillation of the cross-stream vortices, portrayed in Fig. 3a, results in a circumferentially-periodic flow structure. The midplane distribution of the modulus of vorticity, plotted in Fig. 4 for the same 3D calculation of Fig. 3, illustrates the circumferential periodicity with a wave-number $m = 4$.

Predictions for a parameter of practical relevance such as the disk momentum coefficient, C_M, are presented in Fig. 5. The disk momentum coefficient is proportional to the sum of the contributions from each opposing disk surface to the total torque (see reference [8] for further details.) Thus, C_M would give a good idea, in a real computer hard disk consisting of a stack of disks in a casing, of the dissipation of energy due to the rotation of the disks. As can be seen in Fig. 5, predictions from both 2D [14] and 3D calculations agree well with previous experiments of Hudson and Eibeck [15] at the highest Reynolds number investigated. Moreover, calculated C_M values tend to the theoretical behaviour [16] $C_M \propto Re^{-0.5}$ for sufficiently high Reynolds numbers. It should be noted that the -0.5 exponent in the above dependence can only be achieved at Reynolds numbers typically above $Re = 10^5$, when the disk boundary (Ekman) layers are already perfectly established [17].

Acknowledgements

References

[1] Humphrey, J. A. C., Chang, C. J., Li, H., and Schuler, C. A. 1991. Unobstructed and obstructed rotating disk flows: a summary review relevant to information storage systems. Adv. Info. Storage Syst. 1:79-110.

[2] Duck, P. W. 1986. On the flow between two rotating shrouded disks. Computers & Fluids 14:183-196.

[3] Chang, C. J., Schuler, C. A., Humphrey, J. A. C., and Greif, R. 1989. Flow and heat transfer in the space between two corotating disks in an axisymmetric enclosure. ASME J. Heat Transfer 82:217-232.

[4] Schuler, C. A., Usry, W., Weber, B., Humphrey, J. A. C. & Greif, R. 1990. On the flow in the unobstructed space between shrouded corotating disks. Phys. Fluids A 2:1760-1770.

[5] Lenneman, E. 1974. Aerodynamic aspects of disk files. IBM J. Res. Develop. Nov:480:488.

[6] Humphrey, J. A. C., Schuler, C. A., and Webster, D. 1995. Unsteady laminar flow between a pair of disks corotating in a fixed cylindrical enclosure. Phys. Fluids 7:1225:1240.

[7] Abrahamson, S. D., Eaton, J. K. & Koga, D. J. 1989. The flow between shrouded corotating disks. Phys. Fluids A 1:241-251.

[8] Herrero, J., Giralt, F., and Humphrey, J. A. C. 1996. Structural characteristics of the isothermal flow between corotating disks in fixed enclosures. Submitted to J. Fluid Mechanics.

[9] Treidler, E. B. 1991. An experimental and numerical investigation of flow past ribs in a channel. Ph. D. Thesis, University of California at Berkeley.

[10] Tatsutani, K., Devarakonda, R., and Humphrey, J. A. C. 1993. Unsteady flow and heat transfer for cylinder pairs in a channel. Int. J. Heat Mass Transfer 36:3311-3328.

[11] Tatsutani, K., Usry, W. R., and Humphrey, J. A. C. 1992. Numerical calculation of two-dimensional laminar flow and heat transfer for a backward-facing step using Cuteflows. Benchmark Problems for Heat Transfer Codes, HTD-222:1-6 (editors B. Blackwell and D. W. Pepper, ASME Winter Annual Meeting, Anaheim, California.)

[12] Iglesias, I., Humphrey, J. A. C., and Giralt, F. 1993. Numerical calculation of two-dimensional, buoyancy-assisted flow past a backward-facing step in a vertical channel. Computational Aspects of Heat Transfer, Benchmark Problems, HTD-258:63-72 (editors B. F. Blackwell and B. F. Armally, ASME Winter Annual Meeting, New Orleans, Louisiana.)

[13] Schuler, C. A. 1990. Investigation of the flow between rotating disks in an enclosure. Ph. D. Thesis, University of California at Berkeley.

[14] Herrero, J., Humphrey, J. A. C., and Giralt, F. 1994. Numerical investigation of the coupled flow and heat transfer between corotating disks in cylindrical enclosures. Computer Mechanics Laboratoy Technical Report No. 94-002, Department of Mechanical Engineering, University of California at Berkeley.

[15] Hudson, A. J. and Eibeck, P. A. 1991. Toque measurements of corotating disks in an axisymmetric enclosure. ASME J. Fluids Engn. 113:648-653.

[16] Humphrey, J. A. C., Schuler, C. A., and Iglesias, I. 1992. Analysis of viscous dissipation in disk storage systems and similar flow configurations. Phys. Fluids A 4:1415-1427.

[17] Daily, J. W. and Nece, R. E. 1960. Chamber dimension effects on induced flow and frictional resistance on enclosed rotating disks. ASME J. Basic Engn. 82:217-232.
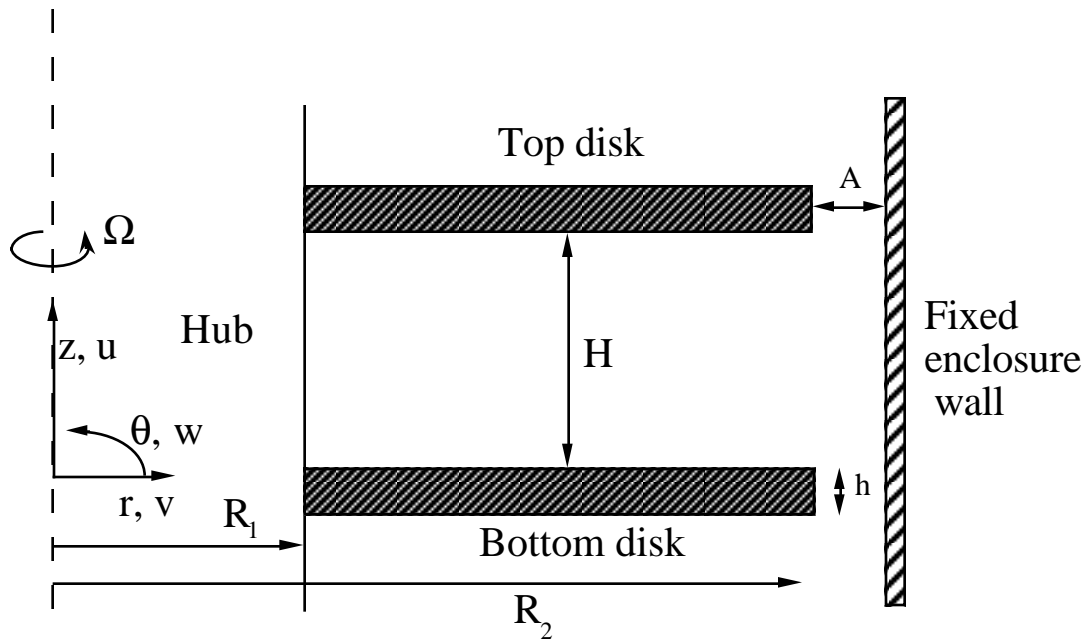
Figure 1: Schematic of the ECDP geometry investigated. Dimensional values are, for the case presented here, H = 9.53 mm, R_1 = 56.4 mm, R_2 = 105 mm and A = h = 0.
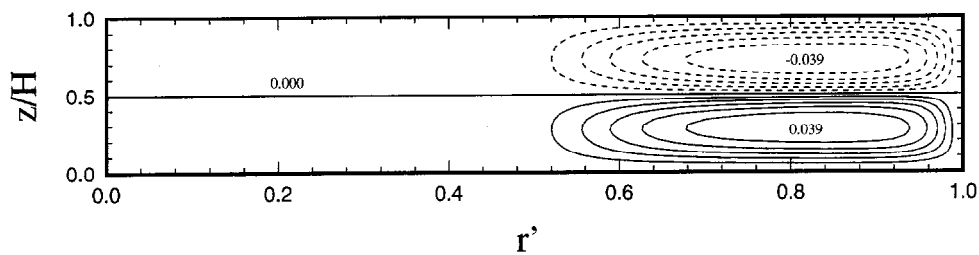

Figure 2: Streamline patter for a two dimensional calculation at Re = 13,710 (Ω = 200 rpm) on a 40x74 (z, r) computational grid. The number of equally spaced iso-contours is 11 with maximum and minimum dimensionless values of -0.039 and 0.039. Negative values (excluding zero) are denoted by dashed lines. The dimensional values of the stream-function have been normalised with the value of the circumferential flow rate that would be crossing the z-r plane at any instant for the case with all the fluid rotating in solid body rotation with the disks and hub.
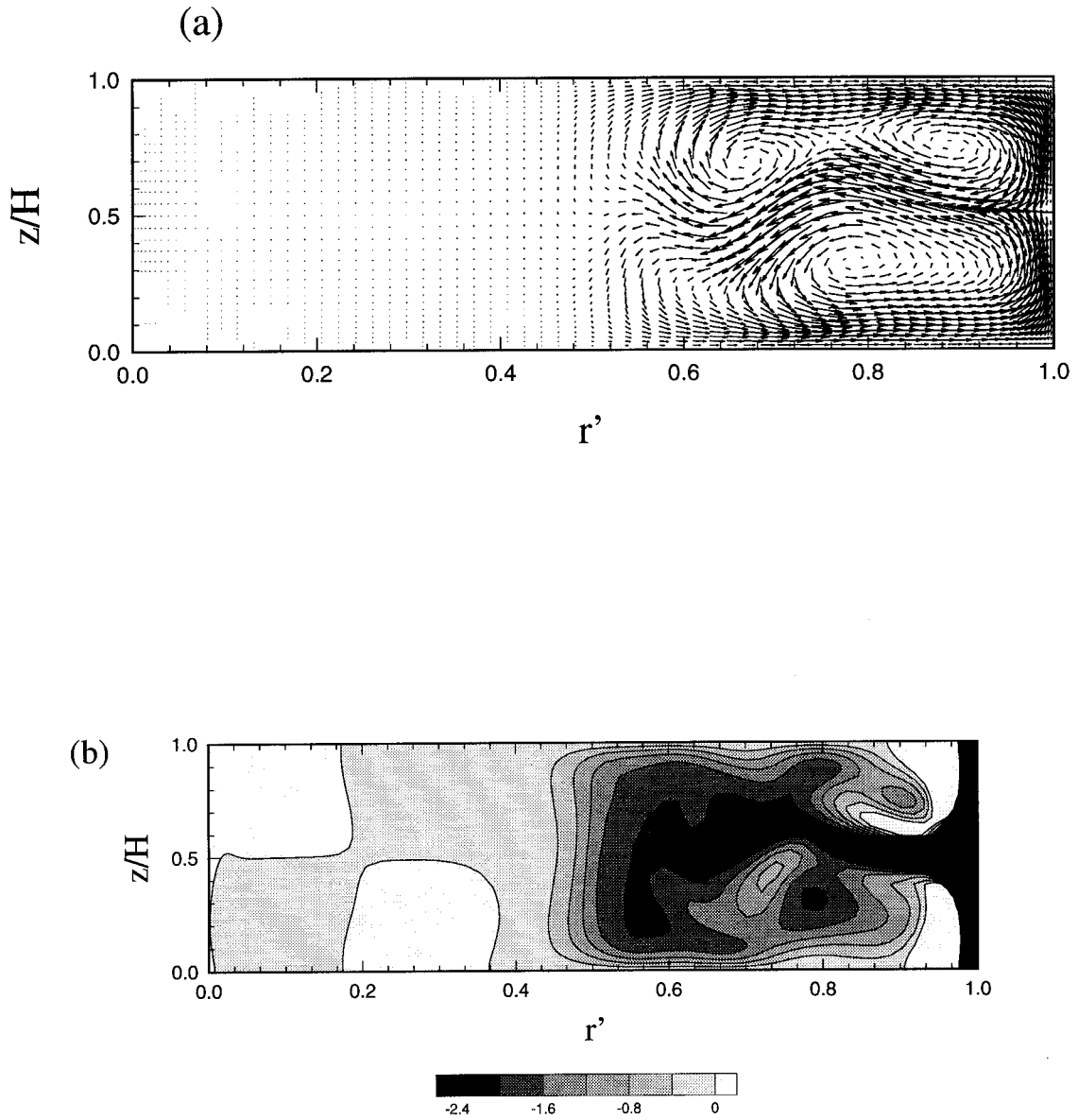
(a)

(b)

Figure 3: Results for a 3D calculation at Re = 20,565 (Ω = 300 rpm) on a 40x74x52 grid. Instantaneous velocity vectors in the cross-stream plane are plotted in (a) while the corresponding distribution of the dimensionless axial component of vorticity is plotted in (b).
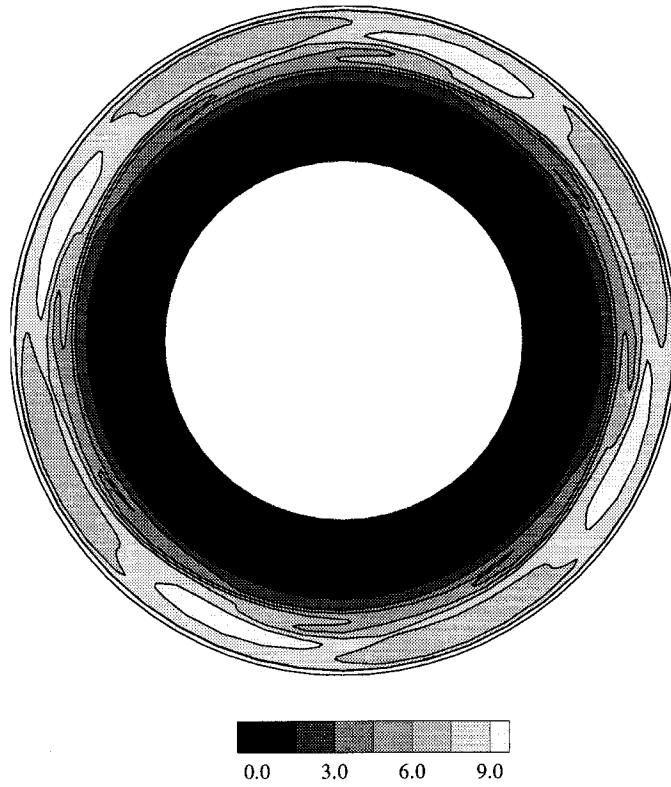
Figure 4: Distribution of the dimensionless modulus of vorticity at the inter-disk midplane for the same 3D calculation of Fig. 3.
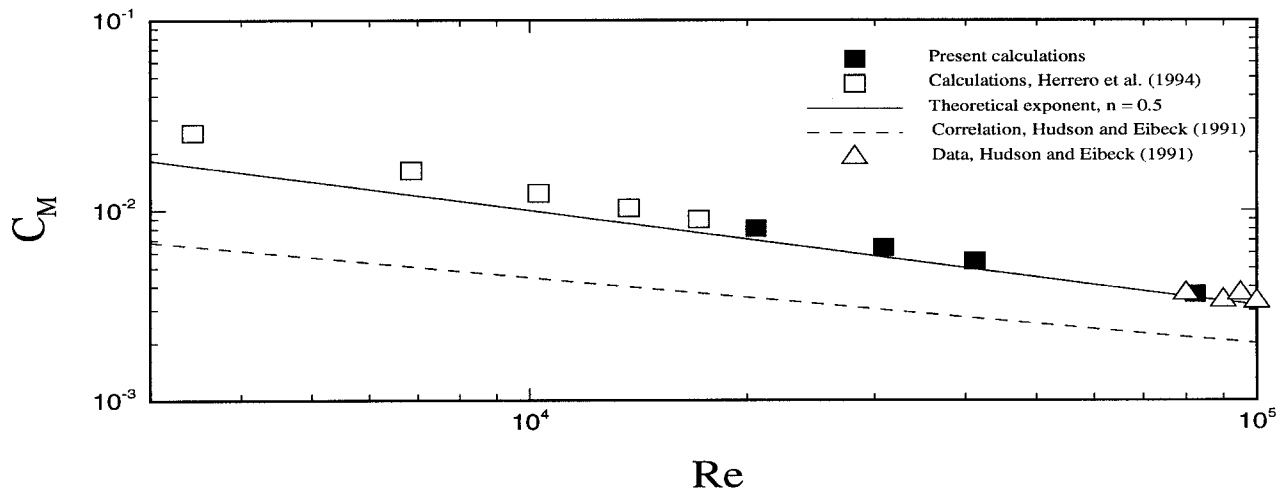

Figure 5: Predicted values of the disk momentum coefficient for different Reynolds numbers. Data by Hudson and Eibeck [14] have also been included for comparison purposes.